Effect of Tensile Strain Rate on the Mechanical Properties of Polystyrene and High-Impact Polystyrene

MITSURU YOKOUCHI, HARUJI UCHIYAMA, and YASUJI KOBAYASHI, *Department of Industrial Chemistry, Faculty of Technology, Tokyo Metropolitan University, Fukazawa, Setagaya-ku Tokyo 158, Japan*

Synopsis

The dependency of the mechanical properties (Young's modulus, maximum load, breaking strain, and breaking energy) of polystyrene (PS) and high-impact polystyrene (HIPS) on the tensile deformation speeds was examined without changing the mode of deformation or the shape of the test specimen. It was found that HIPS has an excellent mechanical balance compared with PS for both low (1.7×10^{-4} to 2.9×10^{-2} m/sec) and high (1.3–16 m/sec) speeds. This is due to the following two mechanisms (which have different time responses) originating from the dispersed rubber particles: (1) at low speeds, the generation of large numbers of microcrazes, and (2) at high speeds, tensile-orientation hardening of the rubber and cold-drawing of the PS matrix resulting from the rise in temperature accompanied by the abrupt elongation of the rubber phases.

INTRODUCTION

Mechanical properties of plastic materials have been examined over a wide range of strain rates from low to high (impact) speeds. There are, however, few published measurements on the effect of rate of extension in tensile-rupture tests. For high-impact speeds most of the experiments have been performed under cantilever impact conditions. Comparison of results, however, for various experiments have proved difficult because the values are very sensitive to the conditions for the preparation of the test piece and the capability of the particular apparatus used. In addition, finding correlations between low-speed tensile and high-speed flexural properties is troublesome because of the differences of the test piece shape and the mode of deformation (tension and flexure). Therefore, there is a need for a systematic apparatus where the tensile breaking tests can be performed over a wide range of strain rates without changing the mode of deformation or the shape of the test specimen. The problem has been the paucity of the appropriate apparatuses where tests could be made efficiently under the speeds of 1–10 m/sec, i.e., impact tensile speeds. Thus, we have designed and fabricated a new flywheel-type, high-speed tensile tester for specimens of polymeric sheet and film.[1,2] When this apparatus and the conventional low-speed tensile machine are used, the strain rate is covered within the range of 1.7×10^{-4} to 26 m/sec.

In the present study, attempts have been made to measure the strain rate dependencies of the tensile mechanical properties of polystyrene (PS) and high-impact polystyrene (HIPS). Generally, plastics in the glassy state (e.g., PS) have excellent stiffness and are used widely as structural materials, but they are not immune from brittle fracture. Studies for the improvement of this

Journal of Applied Polymer Science, Vol. 25, 1007–1015 (1980)

0021-8995/80/0025-1007$01.00

brittleness have been made extensively by introducing sub or pseudosub glass transitions far below practical-use temperature. These include (1) part-modification of the chemical structure of the monomer, and (2) incorporation of dispersed rubber particles. The plastic, HIPS, is a good example of the latter (a solution grafting of rubber in the presence of polymerizing styrene). Several comprehensive reviews have been devoted to the synthesis and physical properties of rubber-modified glassy polymeric materials.[3–5] It was expected that the results obtained by the tensile tests of HIPS and PS (as matrix of HIPS) over a wide range of strain rates could give some insight into the role of dispersed rubber particles in the toughening mechanism.

EXPERIMENTAL

Specimens

Granules of general-purpose atactic PS (Styron 666, Asahi Dow, T_g 95°C) were compression molded (50 kg/cm^2 and 160°C) into sheets of thickness ~250 μm, followed by quenching in ice water. A similar procedure was adopted for granules of HIPS (Styron 470, Asahi Dow, T_g 85°C) except for the compression-molded temperature, which was 150°C. Figure 1, a transmission micrograph of a section microtomed from a stained specimen of HIPS, shows the distribution state of the dispersed rubber particles from which PS is occluded.

Specimens for tensile testing (5 × 90 mm) were prepared from the defect-free compression-molded sheets. A heated cutter was used to prepare specimens in order to avoid cracks at the cut plane. Since both ends were reinforced by aluminum adhesive tape, the practical specimen dimensions were 5 × 58 mm. The specimens were used for both low and high (impact) speed tensile testing.

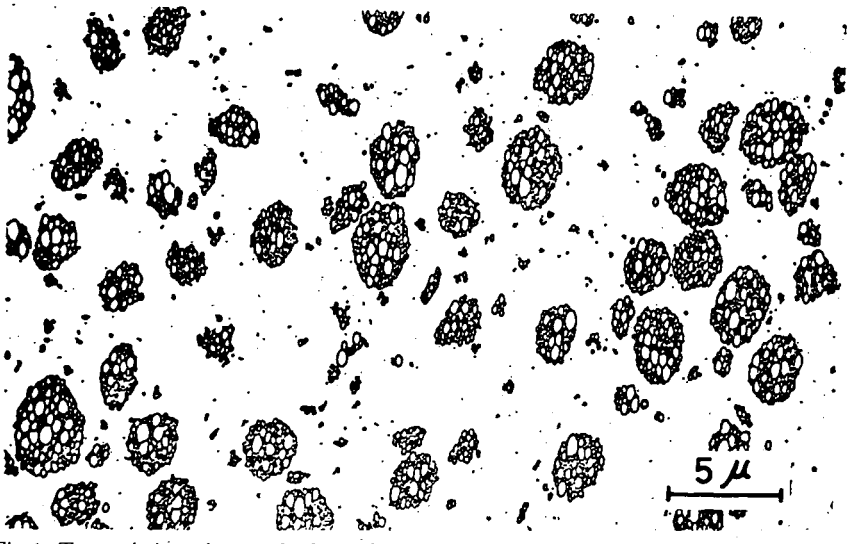

Fig. 1. Transmission micrograph of a section microtomed from a stained specimen of HIPS (Styron 470).

Tensile Breaking Tests

For high-speed tensile testing, a flywheel-type tensile impact tester was used.[1,2] The tensile speeds were controlled by changing the revolutions of the flywheel and in the present study were in the range of 1.3–16 m/sec. For low speeds, a conventional tensile tester was utilized, which covered the rate of deformation from 1.7×10^{-4} to 2.8×10^{-2} m/sec. This enabled us to test over five decades of strain rate (1.7×10^{-4} to 16 m/sec = 0.29–2.8×10^{4} %/sec). The experiments were conducted at almost constant temperature 23 ± 1°C and below 50% relative humidity. The numbers of specimens tested per each strain rate were 10 for the high speed and 5 for the low speed (owing to the small scattering of data points), and the arithmetic mean and estimated standard deviation were calculated from the set of observations.

RESULTS AND DISCUSSION

The voltage–time curves were obtained from the low- and high-speed tensile tests. These curves were easily converted to the stress–strain curves by corrections using the voltage–stress calibration curve, the cross sections of the specimens, and the tensile speeds. Figures 2(a) and 2(b) show the schematic stress–strain curves of HIPS and PS sheets at the deformation speed of 2.8×10^{-3} m/sec and the definitions of five mechanical quantities: (1) modulus of elasticity, E; (2) tensile stress at yield, σ_y; (3) tensile stress at break, σ_b; (4) true strain until failure, ϵ_b; and (5) breaking energy indicated by the area under the curve, S_b. The families of stress–strain curves of HIPS (Fig. 3) are affected by the rate of extension from 1.7×10^{-4} to 16 m/sec. This clearly indicates the existence of strain rate dependency. In contrast, the typical brittle manner of PS did not change during the entire range of strain rates. Hereafter, the discussions of the tensile breaking properties of HIPS and PS from low to high speeds proceed with the above-described four mechanical quantities: E, σ_m (σ_y or σ_b), ϵ_b, and S_b.

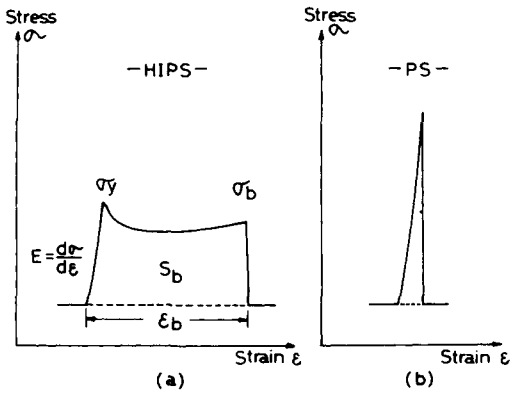

Fig. 2. Typical stress–strain curves of HIPS and PS, and definition of five mechanical properties (E, σ_y, σ_b, ϵ_b, and S_b).

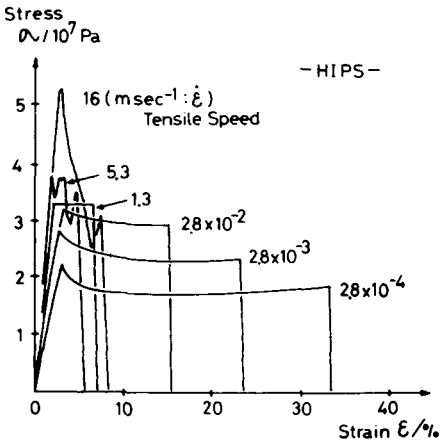

Fig. 3. Families of stress–strain curves of HIPS affected by tensile speeds.

Modulus Elasticity

The strain rate dependencies of elastic moduli plotted against the logarithm of the strain rate are shown in Figure 4. Both PS and HIPS gave a similar variation pattern: E increases very moderately with strain rate in the low region, and increases progressively from ~1 m/sec and passes through a maximum at 5–7 m/sec. Such a change of E in PS implies that a viscous flow mechanism (molecular relaxation process) must be involved at the macroscale even in brittle behavior. This fluidity of molecular chains has been clarified by TEM studies under tension as crazing, where the bands containing many fibrils, a few 10 nm in diameter, are formed at right angles to the major principal stress.[6–9] However, E starts to decrease rapidly at about 5–7 m/sec. This implies that there exists a limitation of molecular fluidity at very high speeds and that microcracks (not crazes) are induced from the beginning.

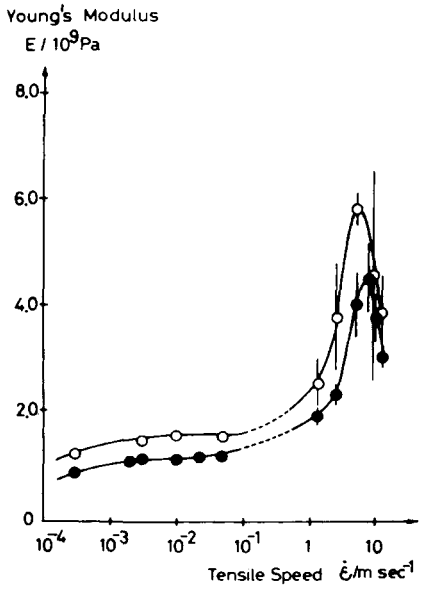

Fig. 4. Strain rate dependencies of elastic moduli E of PS and HIPS. (○) PS, (●) HIPS.

Compared with PS, HIPS has a smaller modulus in the range of 0.3–1.5 GPa over the entire range of strain rate, and the maximum shifts a little toward a higher strain speed. The structural difference is in an imbedding of dispersed rubber particles, which often provide effective sites for craze initiation. The formation of crazes at the rubber–PS interfaces is supported by phase-contrast photomicrographs.[10–14] The results in Figure 4 (E of PS and HIPS) depend on the following factors: (1) molecular fluidity of the PS matrix, (2) stress-concentrating effect of rubber inclusion and the reduced cross section of the load-bearing matrix PS, and (3) the initial similar process of microcraze or microcrack growth into the same PS matrix.

Maximum Load

The strain rate dependencies of maximum loads are shown in Figure 5. As is distinct from the case of E, PS and HIPS give rise to different strain rate dependencies. The maximum load of PS, corresponding to stress at breaking, σ_b, increases slowly with strain rate to a maximum of about 5–7 m/sec. On the other hand, the value of σ_m for HIPS, corresponding to stress at yield σ_y, changes similarly to PS during the low-speed region to the extent of less than about 1/2–2/3 the strength of PS, but increases steeply from about 1 m/sec, followed by a maximum at 10 m/sec. HIPS exhibits a larger tensile strength than PS above the strain rate of 8 m/sec. Increase of σ_m with deformation speed has already been observed in other polymeric materials.[15–18] Moreover, the occurrence of a maximum has been reported in the filled vulcanized rubber (at the strain rate of 6 sec^{-1}, corresponding to 3.5×10^{-1} m/sec if the specimen length is 58 mm).[15]

The dramatic increase of σ_m in HIPS in the high-speed region results from the contribution of dispersed rubber particles. Differing from the initial deformation (which gives information on the elastic modulus), the strain state of

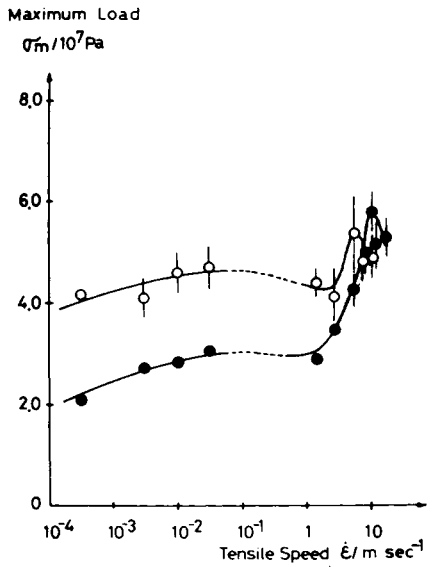

Fig. 5. Strain rate dependencies of maximum loads σ_m of PS and HIPS. (○) PS, (●) HIPS.

the specimen at the maximum load may indicate the following process: microcrazes grow from the boundaries of rubber particles to other rubber particles, then growth is terminated. The craze-stopping efficiency of rubber particles means the elongation of rubber phases. Although the modulus of rubber is approximately 0.001 that of the matrix PS, the orientation hardening cannot be ignored because the affected rubber phases are very thin. This is due to the occlusion of many fine PS particles (Fig. 1), and the relative strain becomes quite large. Therefore, the following factors may be responsible for the increased maximum load of HIPS: (1) the viscoelasticity of rubber during deformation, and (2) the adhesive force between particles and the matrix (in HIPS, provided by a grafting reaction during the manufacturing process).

Breaking Strain

The strain rate dependencies of breaking strain are shown in Figure 6. In the case of PS, ϵ_b is brittle and almost constant over the entire strain rate. In contrast, the elongation of HIPS falls off linearly with the inverse log strain rate in the low-speed region and starts to level off from about 1 m/sec, followed by an abrupt increase at about 7–10 m/sec: Its characteristic is the existence of a minimum, while in the filled vulcanized rubber[15] there exists a maximum as in the case of the maximum load. This breaking strain is closely associated with stress whitening. At the strain rate of 1.7×10^{-4} m/sec, whitening first appears at the yield point over almost the entire specimen and becomes denser in the course of further elongation. With the increase in strain rate, whitening is decreased in density and distributed unevenly in stripes. The higher strain rate (more than 1 m/sec) restrains the whitening band to only one stripe at which fracture takes place. At more than 10 m/sec, whitening becomes more dense. Therefore, breaking strain and stress whitening are different aspects of the same phenomenon.

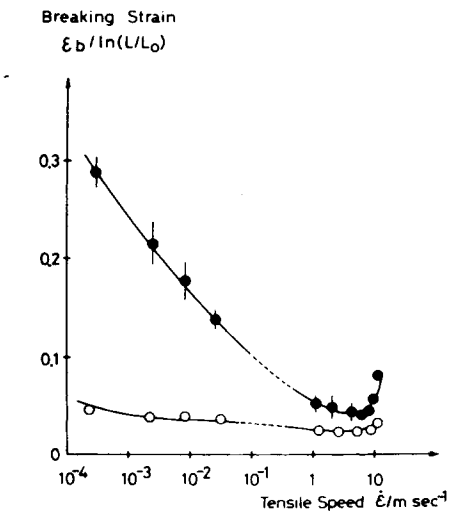

Fig. 6. Strain rate dependencies of breaking strains ϵ_b of PS and HIPS. (○) PS, (●) HIPS.

Whitening is due to the development of craze cracks initiated at the rubber–PS interface.[10,11] However, the relationship between the breaking strain and the strain rate is the reverse of the tendency at low- and high-speed regions, respectively, as shown in Figure 6. A dual reinforcement mechanism exists in HIPS with a different time response: (1) craze and/or crack formation, and (2) separation at the interface of the rubber and matrix.[19–21] The increase in both (1) and (2) is observed as an enlargement of the breaking strain. In the HIPS specimen, there are many groups of rubber particles that have different stress-concentrating abilities. With applied stress, crazes nucleate at the first group of rubber particles, and their growing edges are terminated at other rubber particles, followed by the tensile deformation of the rubber. This tensile-orientation hardening induces the nucleation of crazes at the second group of rubber particles. The slower the strain rate, the longer the time reiterating the above cycle which extends to further groups. This gives rise to an increase of apparent breaking strain. When the deformation speed is higher, however, another mechanism becomes dominant prior to the repetition of the above cycle: the breakdown of the extended rubber and/or the separation of the rubber–matrix interface evolves instantaneously with cracks propagating to rupture. The full extension of the rubber phase has been ascertained by TEM observations of the elongated HIPS films[5,14] and is shown schematically in Figure 7. Therefore, as the quantity of ϵ_b becomes larger, the interfacial adhesive force strengthens: chemically grafted inclusion is of greater advantage than the simple mechanical blend.

The experimental increase of ϵ_b during high-impact strain rate results in part from another mechanism accompanied by the adiabatic deformation of rubber: cold drawing of PS matrix.[22,23] This relates to the flexural impact strength which increases with temperature.[10,14] Cold drawing is explained by both (1) a local heat generation through adiabatic deformation of rubber, and (2) a local increase in free volume (which lowers T_g) as a result of dilation arising from differences

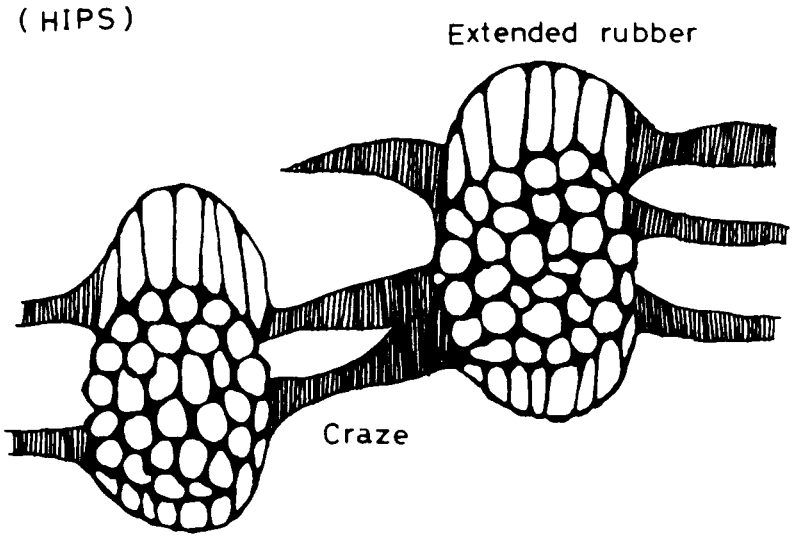

Fig. 7. Schematic diagram representing the deformation morphology (crazes and extended rubber) of HIPS.

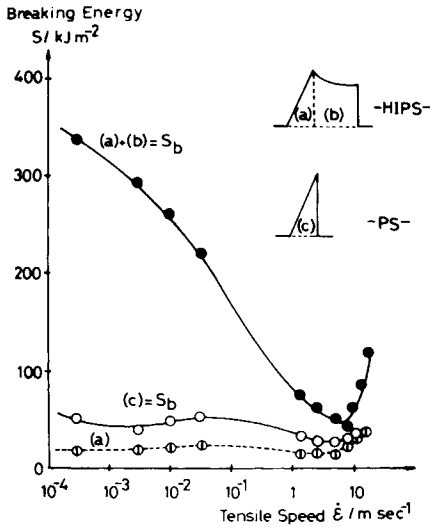

Fig. 8. Strain rate dependencies of breaking energies S_b of PS and HIPS.

in Poisson's ratio of the two phases.[22] In the case of HIPS, the former favors the proposal that the impact blow induces the rubber deformation only at the very thin sphere shell of rubber particles (because of occlusion of many fine PS particles) (Fig. 7).

Breaking Energy

The strain rate dependencies of breaking energy are shown in Figure 8. The patterns almost resemble the case of ϵ_b. The PS value does not change during the entire range of strain rate. In HIPS, the contribution of the elastic deformation region to S_b, curve (a), is small. The value of S_b may be treated adequately as an approximation of the product of σ_m and ϵ_b. While the change in the maximum load is a monotonous increase in the range of 2.0 to 6 GPa (Fig. 5), the breaking strain varies in the relatively wide range of 0.05 to 0.3 and also has a minimum (Fig. 6). Therefore, the product of the two is dominated by the latter. These results indicate that the toughness of PS and HIPS is equivalent to their extension capabilities until fracture.

References

1. M. Yokouchi and Y. Kobayashi, *Rep. Asahi Glass Fund. Ind. Tech.*, **33**, 241 (1978).
2. M. Yokouchi and Y. Kobayashi, *J. Appl. Polym. Sci.*, **24**, 29 (1979).
3. H. Keskkula, *Appl. Polym. Symp.*, **15**, 51 (1970).
4. R. P. Kambour, *J. Polym. Sci. Macromol. Rev.*, **7**, 1 (1973).
5. H. Kawai, *Kobunshi*, **28**, 518 (1979).
6. P. Beahan, M. Bevis, and D. Hull, *Polymer*, **14**, 96 (1973).
7. N. Nakano and M. Kishino, *Sen i Gakkaishi*, **29**, 96 (1973).
8. T. E. Brady and G. S. Y. Yeh, *J. Mater. Sci.*, **8**, 1083 (1973).
9. P. Beahan, M. Bevis, and D. Hull, *Proc. R. Soc. London Ser. A*, **343**, 525 (1975).
10. C. B. Bucknall and R. R. Smith, *Polymer*, **6**, 437 (1965).
11. M. Matsuo, *Polymer*, **7**, 421 (1966).
12. M. Matsuo, *Polym. Eng. Sci.*, **9**, 206 (1969).
13. R. P. Kambour and R. R. Russel, *Polymer*, **12**, 237 (1971).

14. P. Beahan, A. Thomas, and M. Bevis, *J. Mater. Sci.*, **11**, 1207 (1976).
15. H. W. Greensmith, *J. Appl. Polym. Sci.*, **3**, 175 (1960).
16. O. Ishai, *J. Appl. Polym. Sci.*, **11**, 963 (1967).
17. A. E. Moehlenpah, O. Ishai, and A. T. Dibenedetto, *J. Appl. Polym. Sci.*, **13**, 1231 (1969).
18. L. Nicolais and A. T. Dibenedetto, *J. Appl. Polym. Sci.*, **15**, 132 (1960).
19. J. A. Schmitt and H. Keskkula, *J. Appl. Polym. Sci.*, **3**, 132 (1960).
20. J. A. Schmitt, *J. Appl. Polym. Sci.*, **12**, 533 (1968).
21. J. A. Schmitt, *J. Polym. Sci. Part C*, **30**, 437 (1970).
22. S. Newman and S. Strella, *J. Appl. Polym. Sci.*, **9**, 2297 (1965).
23. C. B. Arends, *J. Appl. Polym. Sci.*, **10**, 1099 (1966).
24. M. Matsuo, A. Ueda, and Y. Kondo, *Polym. Eng. Sci.*, **10**, 253 (1970).

Received September 19, 1979